since at the waveguide edges the field profile has nearly disappeared. Again, the fact of having several modes on the LAS is not a drawback as far as its working principles or its possible applications are concerned. An extremely simple way of removing this offset would be placing an absorbent layer at the top of the $d_{1,lat}$ at the end of the waveguide, causing the directional coupler modes to be filtered out.

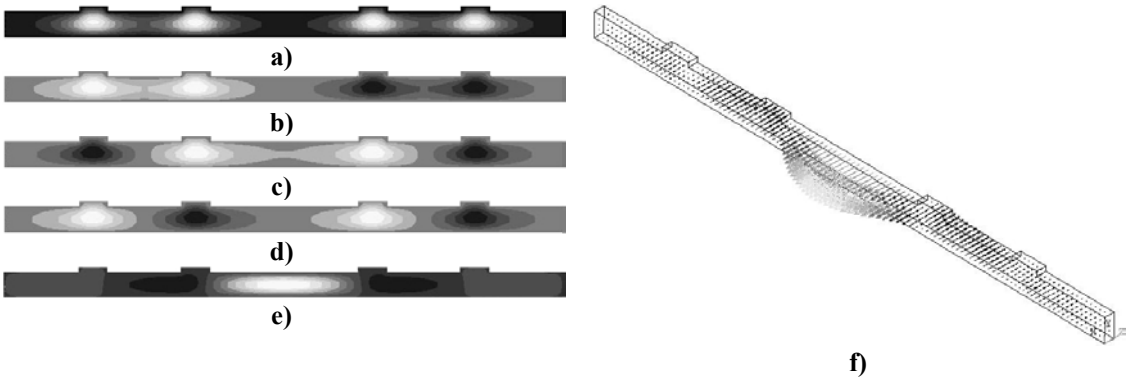

Fig 4.9. Modes in a double ARROW-2D waveguide with d_c=3µm; d_1=0.35µm; d_2=d_c/2; $d_{c,lat}$=15µm; $d_{2,lat}$=$d_{c,lat}$/2, $h_{1,lat}$=0.5µm and $d_{1,lat}$ at its first antiresonant condition. a)-d) double directional coupler modes; e &f) TE_0 ARROW mode.

Optimization of ARROW-2D structures can be summarized with the table 4.2.

Single antiresonant structures

d_c (µm)	d_1 (µm)	d_2 (µm)	n_c	n_1	n_2	$d_{c,lat}$ (µm)	$d_{1,lat}$ (µm)	$d_{2,lat}$ (µm)	$h_{1,lat}$ (µm)	Att (dB/cm)
3	0.35	1.5	1.46	2.00	1.46	8-25	1.9-2.1	$d_{c,lat}$/2	1.5	>0.4

Double antiresonant structures

								x2		
d_c (µm)	d_1 (µm)	d_2 (µm)	n_c	n_1	n_2	$d_{c,lat}$ (µm)	$d_{1,lat}$ (µm)	$d_{2,lat}$ (µm)	$h_{1,lat}$ (µm)	Att (dB/cm)
3	0.35	1.5	1.46	2.00	1.46	6-20	1.7-2.0	$d_{c,lat}$/2	1.5	>0.01

Table 4.2: Optimal dimensions for the ARROW-2D waveguides.

ARROW-2D structures have been shown to be a promising attempt that could allow obtaining large core single mode waveguides. It has been seen that it is possible to design a lateral ARROW structures, by ways of the effective index method, so as to confine light laterally, avoiding rib structures. However, it has to be pointed out that this

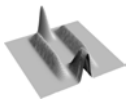

confinement is weaker as compared to rib structures and probably, if a bent ARROW-2D want to be obtained, it would probably require more than two LAS on each side of the waveguide.

4.3 Directional Couplers

Directional couplers have been applied to several aspects of fiber and integrated optics devices, as can be multiplexers **[2]** and filters **[3]**. The effect of having nonlinear couplers has also been studied **[4]**. However, there are some parameters related to its geometry that are seldom considered during its design and that causes a significant variation of its properties.

Only directional couplers based on ARROW structures have been studied. The election of these waveguides arise from the fact that single mode properties are required when using the coupled-mode theory. As it was mentioned in chapter 2, single mode high step index would require extremely small dimensions that would harden the light coupling from a fiber and would dramatically increase the insertion losses. Thus, the device geometry should not only provide with single mode behavior, but also with a relatively good confinement and feasible coupling length.

Firstly, the effect of the device morphology (rib depth, waveguide width and distance between waveguides) will be studied in order to analyze its effect on the main parameter of the directional coupler: the coupling length (L_c). Moreover, it will be seen that having non-completely vertical (90º) waveguide walls, but with a certain tilt causes a reduction of the coupling length. It has to be noted, however, that these parameters under study should be taken into account not only in ARROW-based directional couplers, but also in any evanescent field-based device. Finally, new directional coupler structures will be proposed using ARROW-2D waveguides.

The starting point on the optimization of an integrated optics directional coupler based on ARROW structures requires a previously optimized slab waveguide. We have chosen the ARROW-A and ARROW-B structures proposed in chapter 2 for its fabrication and those are repeated in table 4.1 for clarification. The basic configuration of the directional coupler can be seen in fig. 4.10.

	Δn_{ce}	Δn_{c2}	d_c (μm)	d_1 (μm)	d_2 (μm)
ARROW-A	0.45-0.75	0	3.5-4	0.08-0.14*	$d_c/2$
ARROW-B	0.50-0.60	0	3.5-4	0.3-0.5	$d_c/2$

* (2n+1) multiples of this value are also appropriate

Table 4.1: Optimal ARROW-A and ARROW-B working regions, according to the values obtained, for a fixed wavelength of 633nm.

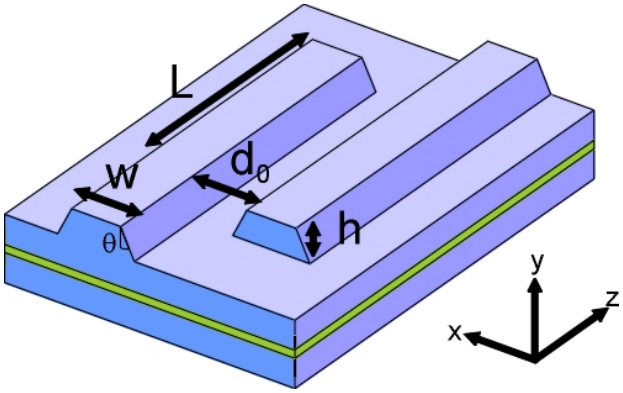

Fig 4.10. Scheme of the directional coupler and the parameters under study: Distance in which both waveguides are parallel (L), distance between waveguides (d_0), rib height (h), waveguide width (w) and wall tilt (θ).

Among all the parameters, the rib height is the most critical, since it is not only the responsible of the light confinement on the waveguides, but also, as it was previously shown, determines the number of lateral modes supported by the rib-ARROW structure. Thus, the coupling length as a function of the rib (h) was firstly analyzed. As it can be seen in fig. 4.11, there is a dramatic increase of L_c as h increases for a given waveguide width (w=4μm, equal in both waveguides) and separation (d_0=3μm) for both ARROW structures, which are in according to the results obtained in **[5]**. This behavior is clearly understood using coupled-mode theory: taking into account that the coupling constant depends on the overlap of lateral evanescent fields, when a stronger confinement of the light inside the waveguide is obtained, a decrease of the coupling constant is straightforward. Thus, it is necessary to reach an agreement between good light confinement inside the core and device total length if feasible dimensions want to be obtained. It can be seen that ARROW-B directional couplers have a slightly lower coupling length for a given rib. This fact can be associated to the increasing overlap of the evanescent field from both waveguides: although the 1st cladding layer in ARROW-B structures has been designed to be thin enough so as to

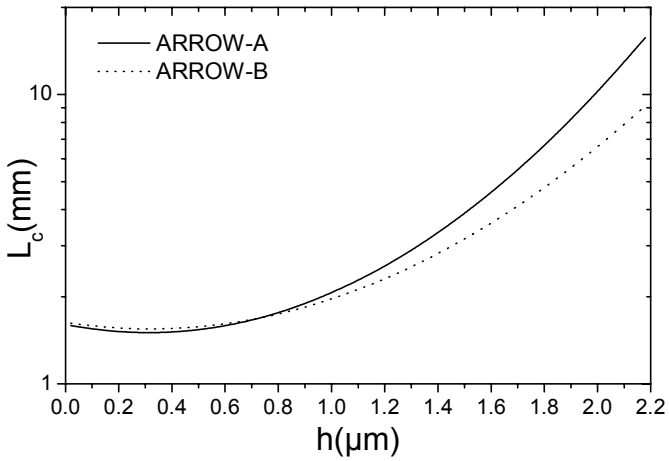

Fig 4.11. Coupling length as a function of the rib height for directional couplers based on ARROW-A and ARROW-B structures. In both cases dimensions where d_0=3μm, w=4μm and the wall tilt θ=90º.

In fig. 4.12, the effects of increasing the distance between the directional coupler waveguides on the dispersion (4.12a), attenuation (4.12b) and coupling length (4.12c for ARROW-A and 4.12d for ARROW-B) is presented. Fig. 4.12a-c are for ARROW-A waveguides. ARROW-B presents an identical behavior and thence its results are not shown. As can be seen, symmetrical and asymmetrical modes of the directional coupler converge, both in effective refractive index and attenuation, to the values that are characteristic of isolated ARROW-A waveguides (see fig. 2.6c). This fact is confirmed by figure 4.12c, where it can be seen that the coupling length sharply increases as the distance between waveguides increase. Generally, waveguides with rib deeper than 1.0μm and distanced more than 15μm can be considered as isolated waveguides. The behavior of the coupling length can be clearly understood if it is considered that, as the distance between the waveguides increases, the evanescent field overlap exponentially decreases, significantly reducing the coupling constant and being necessary an exponentially increasing distance for achieving complete power transference. Moreover, it has to be noted that this behavior is identical for ARROW-A (c) and ARROW-B (d) structures, since in both waveguides the evanescent field is an exponential decay whose

magnitude depends on the core confinement properties. As it was previously described, due to its lower confinement, ARROW-B structures have slightly minor coupling lengths for identical waveguide separation.

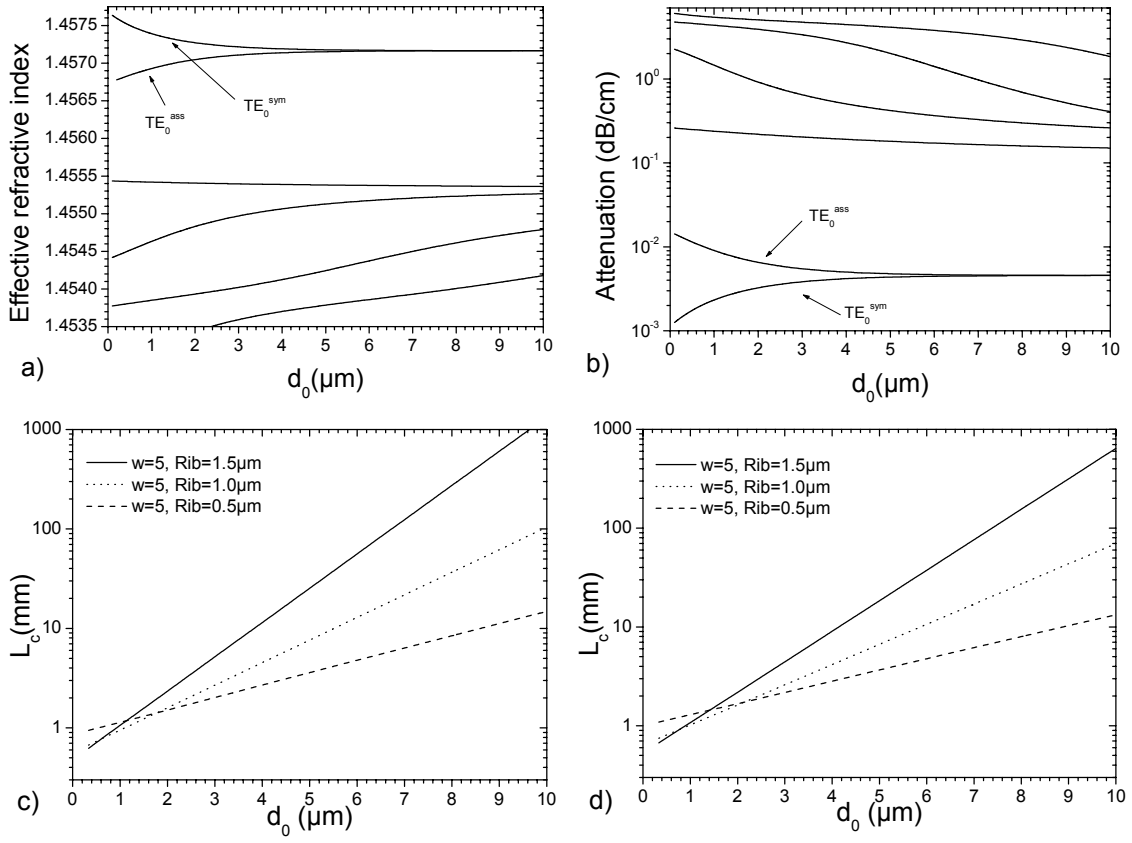

Fig 4.12. Dispersion (a), attenuation (b) and coupling length (c for ARROW-A and d for ARROW-B) as a function of the distance between waveguides (d_0). The wall tilt was fixed at θ=90º waveguide configuration was the optimized in chapter 2.

When analyzing the confinement properties of rib waveguides, it was shown that if waveguide width was progressively reduced, the confinement inside the waveguide would also be lower. This minor confinement causes the evanescent field overlap to increase as the waveguide width decreases, reaching situations were cannot be distinguished between isolated modes of the directional coupler waveguides, but only overall modes of the so-called M-waveguides **[6]**. As it can be seen from the results obtained when studying the coupling length as a function of the waveguide width, shown in fig. 4.13, two different regions can be defined. For very small widths, M-waveguides with non-linear behavior are obtained, since the coupling length increase as

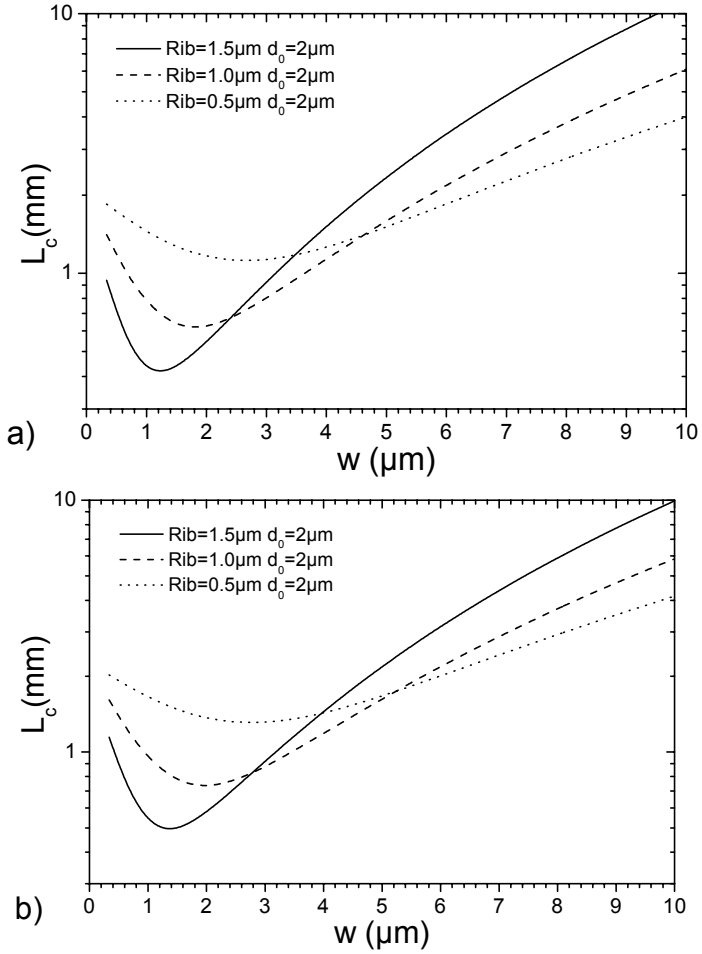

Fig 4.13. Coupling length as a function of the waveguide width (w) in ARROW-A (a) and ARROW-B (b) directional couplers, for different rib height and waveguide separation. The wall tilt was fixed at θ=90º.

Once again, both ARROW-A (a) and ARROW-B (b) directional coupler behaves in identical way, since the coupling properties, as far as confinement is concerned, only depend on the rib, but they do not depend neither on the TIR reflection

at the upper core-air interface nor at the very high antiresonant reflection at the core-1st cladding boundary.

Simulations of integrated optical devices are commonly done by assuming 90º tilt (vertical) waveguide walls since considering the wall tilt on simulations generally causes a dramatic increase of the computing time and hardens its implementation. Although for many integrated optics devices this approximation gives good results, when considering directional couplers there exists an important mismatch between simulation and experimental data due to the fact that a tilted wall does not confine so strongly as it does 90º walls. The tilt on the waveguide walls is inherent on every etching process: it was seen in the previous chapter that wet etching provide, for an amorphous material, 45º tilt walls, which significantly reduces the light confinement and increases its attenuation as compared to 90º tilt walls. Using dry etching techniques, the tilt could vary from the same values of the wet etching to 90º tilt. It has to be noted, however, that the etching conditions are extremely harsh and the layers frequently suffer from an overetching or a non-uniform etching during this process. In our case, we saw that using RIE, it was possible to obtain 80º tilt walls on silicon oxide core layers.

Again, tilted walls effect is not related to the vertical confinement, but to the lateral confinement, thus, both antiresonant configurations will surely have analogous behavior. Hence, only ARROW-B directional coupler results will be presented.

The effect of the wall tilt on the ARROW-B directional coupler symmetric and antisymmetric mode profiles with h=1.5µm, w=5µm and d_0=2µm were studied. As can be seen in fig 4.14, the decrease in the tilt angle causes a modification of the directional coupler modes: The broadening of the symmetrical mode and the slight separation of the lobes of the antisymmetrical mode. This variation can be clearly understood if the AA' cut is done on the contour plots and the coupling length as function of the tilt angle are studied, as is shown in fig 4.14 and 4.15.

At high tilts, the waveguides have the maximum available confinement factor. Hence, the evanescent field is the lowest and, as a consequence, the coupling length has a maximum value. As the tilt decreases, the field adapts its profile to the waveguide morphology and the modes are not so strongly confined, increasing the overlap between the evanescent field of the waveguides. The increasing difference between the effective

index of the symmetric and antisymmetric mode causes an increase of the coupling constant (κ) and thus, the coupling length decreases with the wall tilt, as also shown in fig. 4.16. It can be observed how there nearly exists a 100% difference in the coupling length of two identical directional couplers if their wall tilt differ 45º **[7]**.

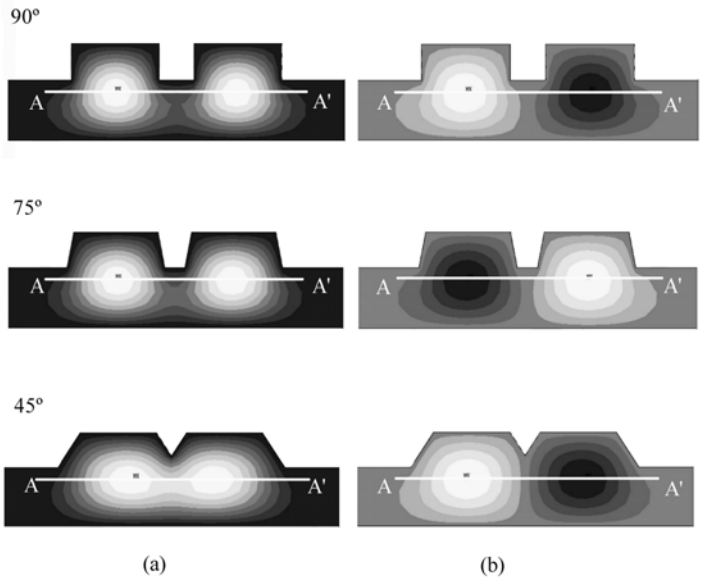

Fig 4.14. Electric Field profile of the symmetric and antisymmetric modes in an ARROW-B directional coupler, for 3 different wall tilt and with h=1.5µm, w=5µm and d_0=2µm.

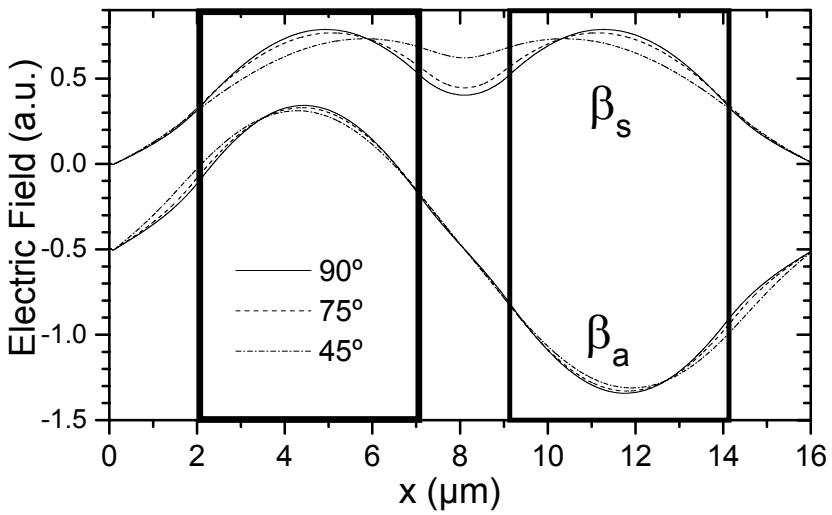

Fig 4.15. AA' cut of the symmetric and antisymmetric modes of fig, 4.14, where the increasing evanescent field overlap of the symmetric mode can be observed, together with the lobe separation of the antisymmetric mode.

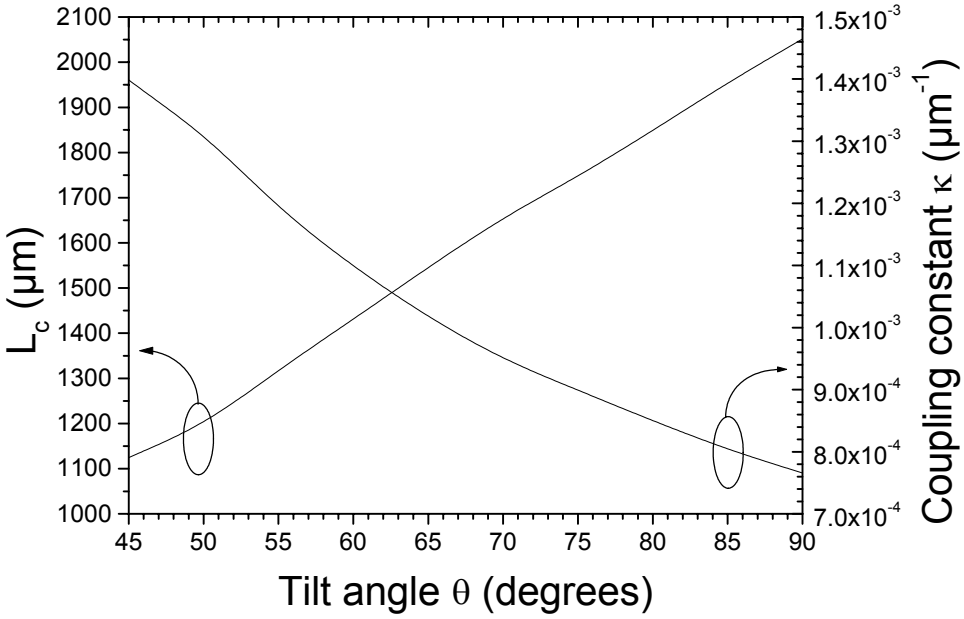

Fig 4.16. Coupling length and coupling constant as a function of the tilt angle for directional couplers with h=1.5μm, w=5μm and d_0=2μm.

Thus, it has been observed that although directional couplers are well-known integrated optics devices, relatively small variations on its morphology could cause a dramatic change in its behavior. Waveguides must be monomode with a relatively low confinement so as to enhance coupling but strong enough so as not to have excessive losses. Separation between waveguides is limited to photolithography precision, which has previously been fixed at 2μm. Excessively separated directional coupler waveguides (>10μm) can be treated as isolated waveguides, since the length at which a substantial amount of power will be transferred to the second waveguide is not feasible. Waveguide width has to be as small as possible in order to reduce the coupling length but width enough so as to allow good light coupling and avoid the non-linear region. Finally, but perhaps the most important parameter, the wall tilt obtained during core definition should be always considered, since it causes large coupling length variations.

Under above mentioned circumstances, a 5μm width has been chosen as optimum for 1.5μm-rib, since it is far from non-linear coupling, has a feasible coupling length and shows monomode behavior in lateral dimension.

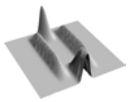

According to previous simulations, optimum dimensions for the ARROW-B directional coupler can be summarized in table 4.2.

Refractive indexes			**Layer thicknesses**			**Directional coupler geometry**				
n_c	n_1	n_2	d_c(µm)	d_1(µm)	d_2(µm)	h (µm)	w (µm)	d_0(µm)	L_c(µm) θ= **90º**	L_c(µm) θ= **80º**
1.54	1.46	1.54	4	0.3	2	1.5	5	2	2052	1848

Table 4.2: Optimal dimensions for the directional coupler.

Finally, in fig. 4.17 BPM simulations of the optimized ARROW-B directional coupler considering 90º walls are presented. Power unity was injected using a Gaussian beam with a beam waist of 4µm, exactly the same shape obtained from a single mode fiber optics. In fig 4.17a it can be seen the expected periodic power exchange as a function of the propagation distance. In order to compare the results obtained by this simulation with those arising by operation of the symmetrical and asymmetrical modes, fig. 4.17a has been transformed to a contour plot, where zones with the same amount of power are plotted with identical gray tone. As can be seen in fig. 4.17b, power is completely transferred to the second waveguide, as it was also expected due to the fact that both waveguides are identical. Coupling length obtained confirms the values presented in table 4.2.

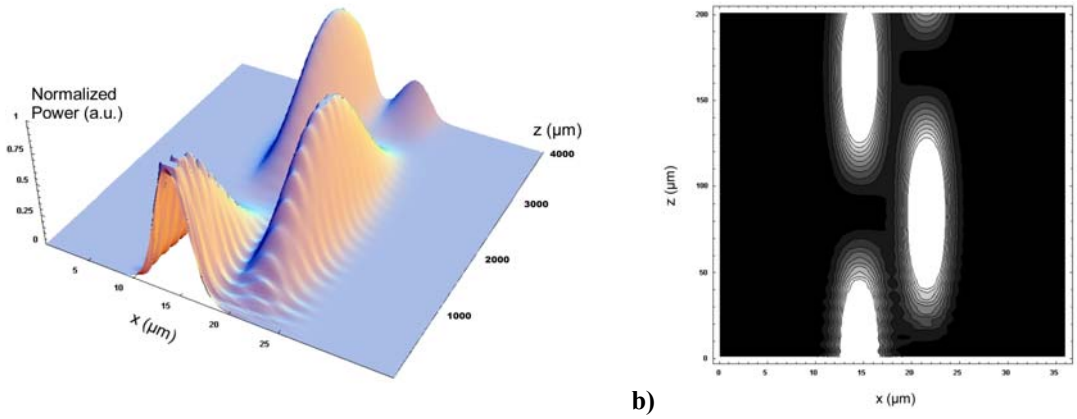

a) **b)**

Fig 4.17. Optimized directional coupler power exchange as a function of the propagation distance when a Gaussian beam is injected to the device. a) 3D plot. b) Contour plot, where the same gray colors identify identical light power values.

We have seen that although feasible, there exist several critical parameters that need high accuracy in order to obtain directional couplers with the expected behavior.

The fact that not only the device dimensions, but also the etching technique cause sharp modifications on the coupling length causes the fabrication requirements to be really strict. Moreover, it has been seen that there exists a very limited range on the device dimensions, both in the waveguide width and distance between waveguides. An alternative approach in order to overcome this latter point is the replacement of rib-ARROW waveguides by ARROW-2D structures, as shown in fig. 4.18. As it can be observed, the basic configuration is identical to a ARROW-2D structure with double lateral antiresonant pairs. Difference arises from the fact that light is injected not into the central region, but in one of the waveguides that belong to the directional coupler.

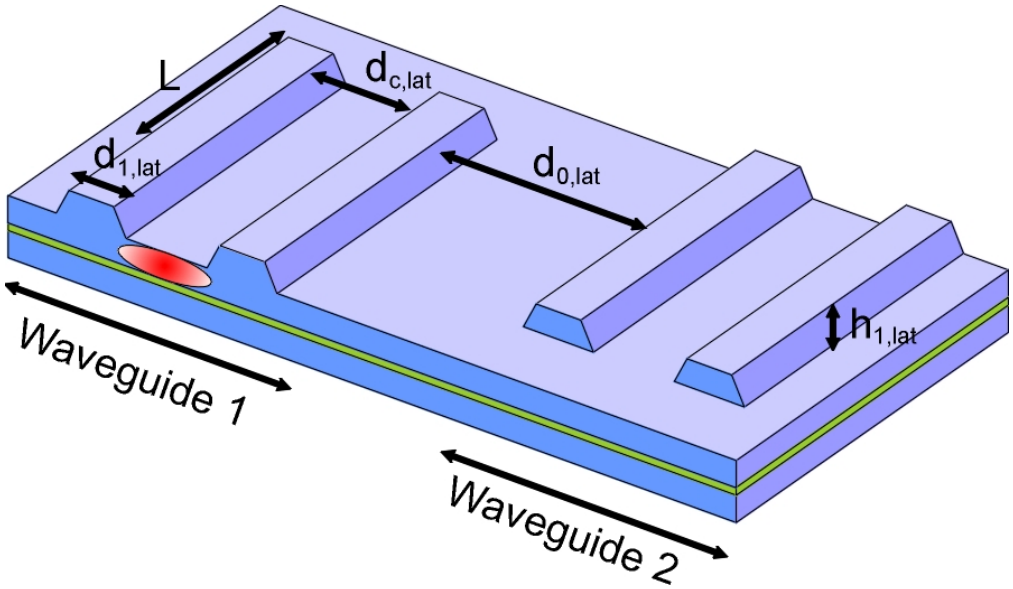

Fig 4.18. Directional coupler based on ARROW-2D waveguides.

From the results obtained in the previous subsection, waveguide lateral dimensions were chosen to be $d_{c,lat}$=12μm, $d_{1,lat}$=2μm and $h_{1,lat}$=1.5μm. Effective refractive index, attenuation and coupling length of the modes as a function of the distance between waveguides are shown in fig. 4.19 (a), (b) and (c) respectively. Significant differences as compared to standard directional couplers can be observed. Firstly, in the rib-ARROW directional coupler, it was shown that the symmetrical and asymmetrical directional coupler modes monotonously tend to the effective refractive index of the isolated waveguide as the distance between them increases. For the structure presented in fig. 4.18, effective refractive index of the overall modes also tends

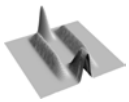

to these of a slab ARROW but they have small flat regions where the modes corresponding to the ARROW-2D waveguides, are coupled forming the symmetric and asymmetric modes of the directional coupler. It can be seen that the different modes of the overall structure are only coupled during a certain region, out of which remain uncoupled. Hence, modes of the ARROW-2D waveguide are successively coupled and uncoupled as the distance between waveguides increases. This fact causes that the coupling length (shown in fig 4.19c), does not increase as the distance between waveguides increase, as it was the case for rib directional couplers, but has a periodical behavior. Therefore remote coupling can be performed, as it was observed in **[8]** and **[9]** in which LAS were defined over a TIR waveguide, forming what the authors called strip-ARROW waveguides. For certain waveguide separations, the whole structure acts as a single ARROW-2D structure with core width $d_{0,lat}$, double LAS pair and $d_{2,lat}$ at its second antiresonant condition in the pair closest to the core while tuned at its first condition in the outer pair. In order to clarify the behavior of such structure, it could be supposed that light is coupled in waveguide 1. Under the previously mentioned parameters, power will be transferred to $d_{0,lat}$, where it will be confined, due to the antiresonant condition of all lateral structures. Thus, when the whole structure acts as an ARROW-2D, directional coupler has a maximum on its coupling length (fig. 4.19c). This fact is logical since both structures have, in this case, the same configuration but opposite behavior: while waveguides are primarily focused on confining light, directional couplers transfer light between waveguides. The opposite case occurs when d_0 has the lateral size by which lateral structures are resonant. Then, fast transition to the second waveguide is produced since $d_{0,lat}$ does not have the required confinement properties and a minimum in the coupling length is obtained.

The most significant example of the remote coupling using ARROW-2D based directional couplers waveguides is presented in fig. 4.20. Distance between waveguides were 96μm. At that distance, two rib waveguides are considered as uncoupled. As can be seen, it is possible to transfer light from the input waveguide to the output waveguide by ways of leaky waves.